Design proposal and optimization potential for an electric drive motor in a 50 PAX hybrid-electric regional aircraft application

M.Meindl[1], XJ. Liu[2], F. Hilpert[2], Valerio Marciello[3], Mario Di Stasio[3] and M. Maerz[1]
[1] Friedrich-Alexander-Universität Erlangen-Nürnberg, Institute of Power Electronics, Germany
[2] Fraunhofer Institute for Integrated Systems and Device Technology IISB, Germany
[3]University of Naples "Federico II", Department of Industrial Engineering, Italy

***Abstract*-- Electric propulsion systems are considered one possibility to reach the ambitious goals of the European Union's Flightpath 2050 concerning greenhouse gas emissions and noise. This paper proposes an engineering architecture design of an electric motor for a propulsion system in a hybrid-electric regional aircraft. The project partners defined the performance requirements for the thrust of the propulsion system. The electric drive motor for the propellers was calculated and then simulated. The motor is specified in this paper, with the materials possible for construction.**

***Index Terms*—electric motors, hybrid-electric aircraft, future propulsion systems, electrification**

I. Introduction

For a hybrid or all-electric aircraft application, motor efficiency and power density to keep the motor weight as low as possible are more important than costs. The battery size can be reduced as motor efficiency increases, allowing weight savings. Considering the crucial role played by weight, permanent magnet synchronous machines (PMSM) are the most suitable option for electric propulsion in hybrid electric aircrafts. For further research studies, hydrogen will be stored in the aircraft. Using partially (i.e. only with a superconducting rotor) or fully superconducting externally excited synchronous machines is possible with liquid hydrogen. Propellers, a gearbox and electrical machines drive the regional aircraft. PMSMs are a type of electrical machines [1]. The machine's weight is reduced by replacing the rotor windings with permanent magnets, resulting in better power density. In addition, the excellent efficiency, high torque-to-inertia ratio and high torque-to-volume ratio of PMSMs have led to their wide application in the aerospace industry. Accordingly, this paper proposes a PMSM for the aircraft's first hybrid-electric propulsion system. Although PMSMs offer the above advantages, they need to evolve with existing technology to meet the requirements of an all-electric aircraft. Thus, the transition to all-electric aircraft requires machines that deliver sufficient power. The machines must be powerful, and at the same time, the machine's weight must be kept as low as possible. These requirements necessitate changing the machine structure, combining new materials and better cooling techniques. Current optimization solutions for the structure of the electrical machine, such as Halbach array and slotless machines, increase the performance of the electrical machine by improving the air gap flux density or the current coating [2]. This work presents an application of innovative solutions for a future regional aircraft concept, with entry into service year 2030, whose hybrid-electric architecture features two electric generators (referred to as primary machines) and eight distributed propellers driven by as many electric machines (referred to as secondary machines). The aircraft was designed as part of the Clean Sky 2 GENESIS project (Gauging the ENvironmEntal Sustainability of electrIc aircraft Systems) [3].

In chapter II, a description of the architecture as well as the physical model underlying the modeling of electric machines is given. In chapter III, the main results of the design activity are reported, with emphasis on the configuration choices and on the results of a simulation of the behavior of the machines. In chapter IV the optimization opportunities are discussed in more detail with reference to new materials, the use of Halbach arrangement of permanent magnets and directly cooled stator windings. Finally, chapter V draws the conclusions of the work.

II. Electric drive system

As it will be discussed in chapter III in more detail, for the application reported in this paper, the considered power demand of the electric machines is 554 kW for each secondary machine and 1108 kW for the primary machine. The secondary electrical machines always have half the power requirement of the primary electrical machines. Therefore, it is proposed to reuse the components of the secondary electrical machines in the primary machines. In the primary machines, two secondary machines are stacked on top of each other and connected with a common rotor shaft. This principle is not new. For example, the motor manufacturers EMRAX and MagniX recommend this variant to double the motor power and torque [4, 5]. Fig. 1 shows how such a configuration could look in principle. Not only the secondary motors but also the motor drive inverters for the secondary machines can be reused. Two motor drive inverters are combined as generator drive inverters for the primary motors. Multi-phase motors and inverters are used to ensure fail-safety and limit the power requirements for individual parts [6, 7].

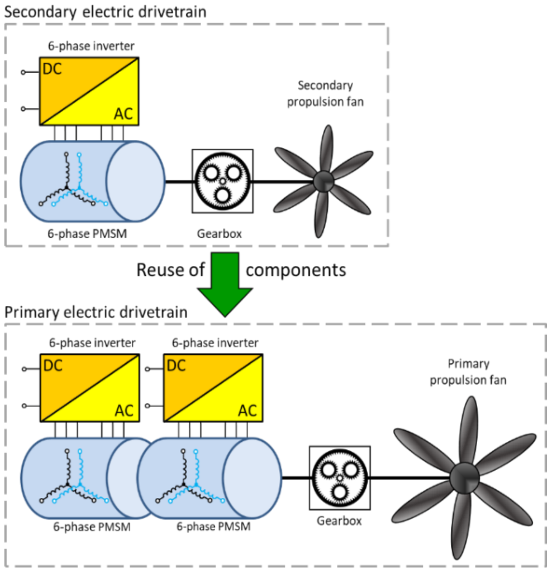

Fig. 1. Reuse of secondary electric drivetrain components to build up the primary electric machine

A secondary machine is a six-phase machine driven by a six-phase motor drive inverter. The primary machine consists of two stacked six-phase machines, each driven by two six-phase motor drive inverters.

A. Conditions for designing electric motors

Maxwell-Equations

Electrical machines are developed based on the application of electromagnetism and, therefore, require an understanding of the properties of electromagnetic phenomena. Maxwell's equations describe the relationship between electric field, magnetic field, electric current and electric charge, so the properties of electromagnetic phenomena are better understood using Maxwell's equations. Maxwell's equations include, in particular, equation (1), (2), (3) and (4) [8].

$$\vec{\nabla} \cdot \vec{E} = \frac{\rho}{\varepsilon_0}. \quad (1)$$

$$\vec{\nabla} \cdot \vec{B} = 0. \quad (2)$$

$$\vec{\nabla} \times \vec{E} = -\frac{\partial \vec{B}}{\partial t} \quad (3)$$

$$\vec{\nabla} \times \vec{B} = \mu_0 \vec{J} + \mu_0 \varepsilon_0 \frac{\partial \vec{E}}{\partial t}. \quad (4)$$

Where E is the electric field strength, B is the magnetic flux density, ρ the charge density, J is the electric current density, ε_0 the permittivity, μ_0 the permeability.

B. Losses in electric motors

The friction losses and also additional losses are neglected here in this work for simplification. The additional losses are, for example, losses in metallic parts outside the laminated core and load-dependent additional losses in the laminated core. In addition to the losses mentioned above, the significant losses in electric motors can be divided into three categories: Winding losses, hysteresis losses and eddy current losses, which are listed below [9].

Winding losses

The winding is one of the most critical components of the electric motor. The amount of winding determines how much electrical power the electric motor can transfer and is usually designed with copper windings. When a current flow through the copper, a part of the electrical energy is lost due to the internal resistance and is converted into heat. This converted energy is called winding losses or current heat losses. Winding losses are among the most critical losses in a conventional electric motor. In the PMSM, winding losses occur mainly in the stator winding, as permanent magnets replace the rotor winding. The winding losses can be described as a function of the electrical resistance and the electrical current with the equation (5) [9].

$$P_{V,R} = Ri^2 \quad (5)$$

Furthermore, the electrical resistance generates heat in the windings. The electrical resistance calculation is possible by using equation (6) as a function of the ambient temperature of 20 °C [10]:

$$R = R_{20°C}[1 + \alpha_{Cu}(\vartheta - \vartheta_{Environment})] \quad (6)$$

Where $R_{20°C}$ is the electrical resistance at ambient temperature, α_{Cu} is the temperature coefficient with a value of $3.93 \cdot\cdot 10^{-3}$ 1/K, ϑ indicates the temperature. The winding losses can be kept at a correspondingly low level by effective cooling methods [10].

Hysteresis losses

The metal of the stator and the rotor consists of soft magnetic material and is demagnetized cyclically in the motor. Hysteresis losses occur due to cyclic demagnetization. The hysteresis losses are material-dependent and proportional to the frequency, the flux density and the volume of the laminated core, as shown in equation (7) [9].

$$P_{V,H} = c_H f \hat{B}^2 V_{Fe} \quad (7)$$

Eddy current losses

According to the law of induction, an induced voltage is generated on an electrically conductive material in a changing magnetic field, resulting in an induced current called an eddy current. This eddy current further generates heat as losses in the material [10, pp. 586-599]. The eddy current losses calculation is possible by using the equation (8) [9].

$$P_{V,W} = c_W f^2 \hat{B}^2 V_{Fe} \quad (8)$$

c_W is a constant and refers to the electrical conductivity of a material. The laminated core is used as the iron core in the stator and rotor to minimize the effects of eddy current losses.

B. Cooling methods of PMSM

Usually, the losses are converted into heat inside the electric motor. If efficient conduction of the heat cannot be out of the electric motor by cooling, it significantly impacts the operation of the electric motor. Therefore, adequate cooling is necessary for the operation of electric motors. Handling the cooling in the motor is possible through three types of cooling methods, conduction (heat conduction), convection (heat entrainment) and thermal radiation (heat radiation) [8, 11].

Conduction

Conduction transfers heat from a higher energy level to neighboring molecules at a lower energy level via lattice vibrations; this heat conduction occurs through intermolecular interactions. Calculating the Conduction between solids, liquids, and gases is possible with the equation (9) [8].

$$\emptyset_{th} = -\lambda A \frac{d\vartheta}{dx} \approx -\lambda A \frac{\Delta\vartheta}{l} \quad (9)$$

Where λ is the thermal conductivity, A is the thermally conductive cross-sectional area, $\Delta\vartheta$ is the temperature difference, and l is the length.

Thermal radiation

Thermal radiation is the transfer of heat by electromagnetic radiation. The main difference between this type of heat transfer and the other two is that thermal radiation does not require a heat transfer medium. The thermal radiation's heat flux density calculation uses the equation (10) [11].

$$q_{th} = \frac{Q_{th}}{A} = \varepsilon\sigma(T_1^4 - T_2^4) \quad (10)$$

A short description of the values in the equation: ε is the emission degree; σ is the Stefan-Boltzmann constant with the value of $5{,}67 \cdot 10^{-8}\, W/m^2K^4$; T_1 is the thermodynamic temperature of the radiating surface; T_2 is the thermodynamic temperature of the absorbing surface.

Convection

Convection is the transfer of heat between an area of higher temperature and an area of cooler temperature that occurs as a result of the movement of the coolant relative to the solid surface. Newton's law governs heat removal by convection with equation (11) [8].

$$q_{th} = \frac{Q_{th}}{A} = \alpha_{th}\Delta\vartheta \quad (11)$$

α_{th} is the heat transfer coefficient. Furthermore, convection can be further divided into two types, forced and natural convection. Due to its excellent cooling properties, forced convection finds its application in many areas.

Therefore, the most useful cooling method is forced convection as a cooling method for the electric motors in the GENESIS project.

C. Power density and design process for the machines

Power density

In the aviation industry, there is always a lot of discussion and comparison about power density. Therefore, this chapter briefly introduces a simple calculation of the power density of electric motors. The design of an electric machine depends on many different parameters like stator current density, magnetic field density, pole pair number, number of slots, rotor diameter, rotor length, and the stator geometry defined by yoke thickness teeth height, and teeth width. The power density is the engine power ratio to engine weight, as given in the equation (12). A higher value of power density means that an engine of the same weight can produce more power. The electric machine's lower weight follows the aircraft's lower weight. Therefore, a lower energy consumption is feasible.

$$\frac{P_m}{m} = k_{geometry} \cdot B_g \cdot A \cdot n_{rot} \cdot \eta_{EM} \quad (12)$$

Where P is the electrical motor power, m is the motor mass, B_g is the magnetic field density in the air gap, A is the stator current density, n_{rot} is the motor speed and η_{EM} is the motor efficiency. The geometry parameters $k_{geometry}$ include, e.g., the geometrical details of the teeth (e.g., width and height) and of the rotor, the winding geometry, etc. The power density is directly proportional to the magnetic field density in the air gap. Therefore, neodymium iron boron (NdFeB) magnets are the best option for the magnet arrangement. They are expensive, but this material has the highest magnetic flux density and thus enables the highest power density. The power density also increases with the stator current density, which is limited by the cooling of the stator. A typical value of 10 A/mm^2 is possible for a water-jacked cooled motor. A value of 25 A/mm^2 is possible with direct liquid-cooled windings. For superconducting machines, the current density can even be more significant than 500 A/mm^2.

However, with higher current density, the ohmic losses of the stator windings also increase, resulting in lower efficiency. A conventional water-cooled motor, presented in the chapter III, is to provide the electric drive for the GENESIS aircraft in this time horizon. This motor provides a basis for further investigations. A high speed has a positive effect on the power density of the motor but a negative effect on the losses of the AC motor. In addition, a higher Pulse-Width modulation (PWM) switching frequency is required, which leads to higher inverter losses. Overall, the efficiency of the motor suffers if the speed is increased too much. This discussion is taken up and evaluated in each chapter and each machine design.

Design process of electric machines

A first estimation of the power demand for the electrical machines was carried out by UNINA (University of Naples" Federico II") and submitted to FAU (Friedrich-Alexander-Universität Erlangen-Nürnberg) to allow the detailed design of the electrical machines for all scenarios. The information provided by FAU on the mass, efficiency and rotational speed of the electric machines was transferred to the model from UNINA for the assessment and implementation of hybrid-electric aircraft. This data exchange resulted in changes to the performance requirements for the electric machines.

The best solution for the power distribution of the electric machines in the hybrid-electric aircraft was found in several iterations and meetings with UNINA. The speed of the electrical machines can generally be adjusted by selecting the gearbox's transmission ratio. The various speeds of the electric machines are adjusted to the speeds of the rotor via the gearbox. A rough machine design and calculation are possible. To determine the exact machine weight and machine performance two tools were necessary. The used tools were ANSYS and CREO Parametric. ANSYS is a simulation software that uses finite element analysis (FEA) to calculate and represent the behaviour of design options. ANSYS Maxwell calculates the electromagnetic behaviour of design options through Maxwell's equations. In addition, robust electromagnetic behaviour is necessary to design an electric motor. Therefore, the built designs are tested cumulatively using ANSYS Maxwell. The software version used is ANSYS Electronics Desktop 2021 R2 [12], and the software version of ANSYS Maxwell is 12.1. Creo Parametric [13] and its extensions provide 2D CAD, 3D CAD, parametric and direct modelling capabilities that allow designs to be created, analysed, viewed and approved for downstream processes.

This section is concluded with an overview of a 50 PAX hybrid-electric aircraft with a gas turbine and battery as an energy source and the drivetrain's arrangement (Fig. 2). The propulsive architecture is based on a serial/parallel partial hybrid configuration with two distinct propulsive lines. This choice made it possible to use distributed electric propulsion during the ground phases to increase the lifting capabilities of the aircraft. In this way, it is possible to compensate for the increased mass and a lower propulsive efficiency associated with the secondary propellers and the hybridization of the energy source.

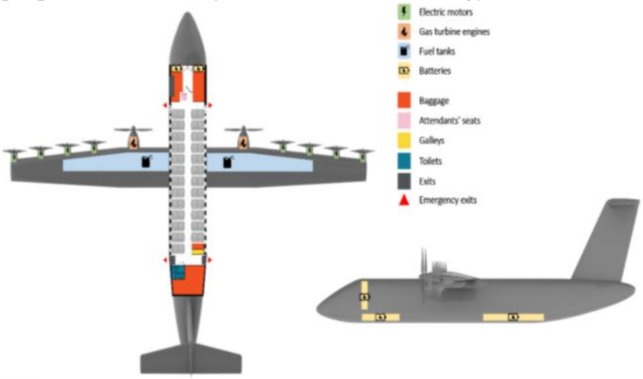

Fig. 2. Schematic view of the aircraft (Gasturbine + Battery) [14]

Directing all the power to the primary shafts during the cruise phase was convenient in order to maximize the efficiency during the most extended phases of the mission when the lift capability requirements are less demanding.

III. Design Analysis results

A six-phase 554 kW liquid-cooled PMSM motor was designed to meet the requirements for the secondary electric machine. The power density is directly proportional to the magnetic field density in the air gap B_g. Therefore, neodymium iron boron (NdFeB) magnets were chosen. This magnet has the higher magnetic flux density and enables the highest power density. The power density also increases with the higher stator current density A, which is limited by the cooling system. For a water-jacked cooled motor, a typical value of 10 A/mm^2 is possible for the rated power. With direct liquid-cooled windings, a value of 25 A/mm^2 can be reached. For the current motor design, presented at the end of the chapter, a conventional water-jacked cooled motor was chosen to have a baseline for future investigations. The gearbox ratio was chosen to 1:10 to limit the motor speed to 14,000 rpm during the "Cruise phase".

The mechanical parameters of the primary and secondary drivetrain are listed in TABLE I [15]. A high rotational speed positively influences the motor power density, but it negatively affects the motor losses.

TABLE I. Mechanical parameters for the secondary and primary drive train

	Use Case	Take off	Climb	Cruise
Primary propeller	Mission time in min	0.34 / 0.37	21 / 24	12 / 97
Primary propeller	$P_{Propeller}$ in kW	340	1266	1136
Primary propeller	$T_{Propeller}$ in Nm	5760	12173	7780
Primary propeller	$n_{Propeller}$ in rpm	564	993	1394
Primary propeller	$\eta_{Propeller}$ in %	63	84	85
Primary motor	$\eta_{Gearbox}$ in %	98	98	98
Primary motor	Gearbox ratio	1:10	1:10	1:10
Primary motor	$P_{Motor,mech}$ in kW	1224	233	209
Primary motor	T_{Motor} in Nm	2074	224	143
Primary motor	n_{Motor} in rpm	5637	9931	13943
Secondary propeller	Mission time in min	0.34 / 0.37	-	-
Secondary propeller	$P_{Propeller}$ in kW	407	-	-
Secondary propeller	$T_{Propeller}$ in Nm	6900	-	-
Secondary propeller	$n_{Propeller}$ in rpm	563	-	-
Secondary propeller	$\eta_{Propeller}$ in %	75	-	-
Secondary motor	$\eta_{Gearbox}$ in %	98	-	-
Secondary motor	Gearbox ratio	1:10	-	-
Secondary motor	$P_{Motor,mech}$ in kW	554	-	-
Secondary motor	T_{Motor} in Nm	939	-	-
Secondary motor	n_{Motor} in rpm	5633	-	-

Moreover, a higher PWM switching frequency is necessary but this will lead to higher inverter losses. Overall, it can be said that if the rotational speed is increased too much, the motor efficiency will suffer. TABLE II shows the design results for the secondary electric machine, considering “Take off” as the reference phase for design. In fact, this is the most crucial operating point, as it has the highest output power demand. The motor efficiency was estimated to be about 96 %. The power density for active parts is about 10.6 kW/kg.

With a total motor weight of 86.5 kg, the total power density is calculated to 6.4 kW/kg. This lies above the state-of-the-art power densities, which are between 2 and 5 kW/kg. The hairpin winding was chosen to increase the power density, achieving a copper fill factor of about 0.60.

TABLE II. RESULTS OF TECHNOLOGY ANALYSIS FOR 6-PHASE SECONDARY ELECTRIC MACHINE FOR “TAKE OFF” POINT

Parameter	Value	Unit
DC link voltage	800	V
Nominal phase current 3-phase	770	A_{RMS}
Nominal phase current 6-phase	385	A_{RMS}
Nominal power	554	kW
Nominal torque	993	Nm
Nominal speed	5633	rpm
Maximum speed	15000	rpm
Estimated efficiency	96	%
Effective length	180	mm
Total length	215	mm
Stator outer diameter / inner diameter	265 / 217	mm
Rotor inner diameter	80	mm
Number of Poles / Slots	1	mm
Number of windings per phase	2	/
Wire cross section	2.91 x 2.3	mm
Magnet dimensions	15.5 x 5.0	mm
Magnet material	G48UH	
Stator material	M270-35A	
Rotor material	M270-35A Hs	
Magnet weight	3.4	kg
Windings weight	5.6	kg
Active parts weight	52.3	kg
Housing weight	18.8	kg
Total weight	86.5	kg
Power density for active parts	10.6	kW/kg
Total power density	6.4	kW/kg

Fig. 3 shows the winding scheme of the secondary electric machine. Fig. 4 shows the final design of the active parts of the secondary electric motor and a closer look at the orientation of the permanent magnets inside the rotor is presented (left). This magnet configuration helps to increase the motor torque. The final design of the active parts of the secondary electric motor is shown on the right in Fig. 4.

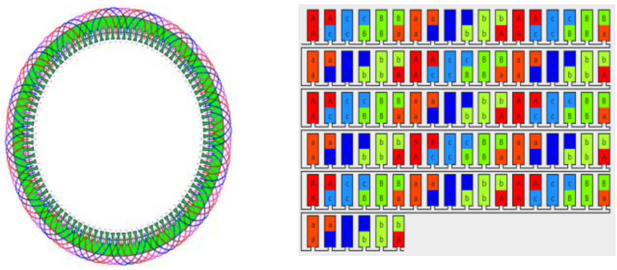

Fig. 3. Winding scheme of the secondary machine.

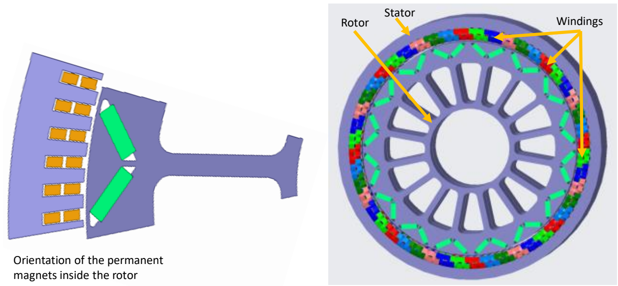

Fig. 4. Orientation of permanent magnets (left) and mechanical design (right).

The electromagnetic design was simulated using FEM software, which enabled simulation of the electromagnetic parameters. The simulation results of the electromagnetic torque and induced voltages are presented in Fig. 5 and Fig. 6.

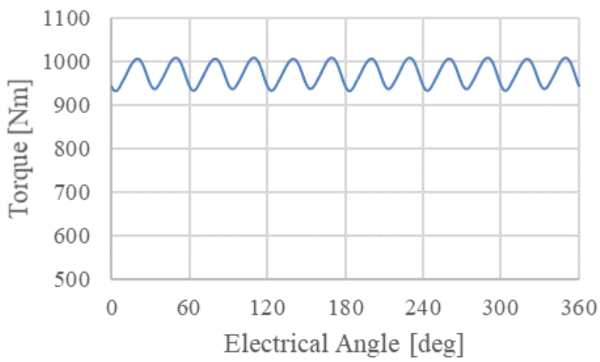

Fig. 5. The simulated torque of the motor from FEM.

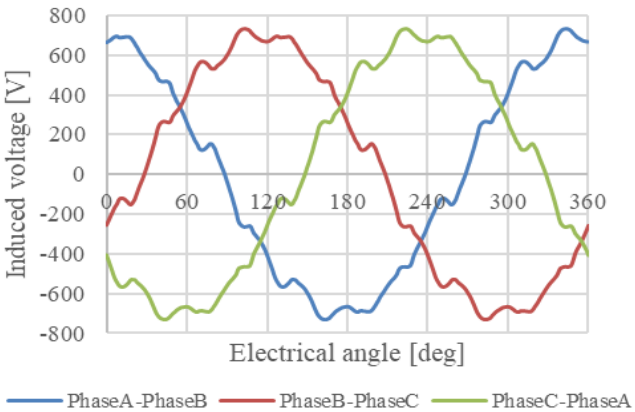

Fig. 6. The simulated induced voltage of the motor.

The combination of stator slots number and pole number in an electric motor can result in the generation of harmonics of the induced voltage. These harmonics can be analyzed using the Fast Fourier Transformation (FFT). The results of the FFT analysis can be visualized in Fig. 7. Due to the slot opening on the stator side, this design can produce high levels of specific harmonics [16]. These harmonics have the potential to increase losses within the motor [17]. In order to address this issue, designing a skewed rotor or a non-uniform air gap should be considered during the motor design process in next steps. These design modifications can help reduce torque ripple, motor losses, and the maximum induced voltage in the stator winding. It is important to carefully evaluate the potential benefits of these design changes against their associated complexity and cost for this specific motor application.

Fig. 8 shows the mechanical motor design with the water-cooled housing, bearings, and rotor shaft. In addition, the mechanical design of the primary electric machine as a stacked version of two electric engines is shown. On the top of Fig. 8 is an assembly of the individual components of one machine visualized.

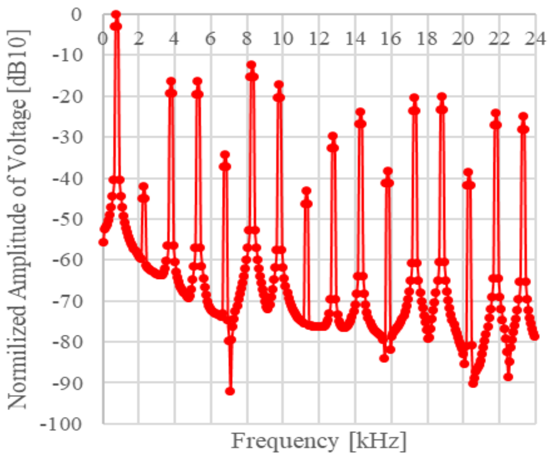

Fig. 7. FFT results of inducted voltage at 554 kW

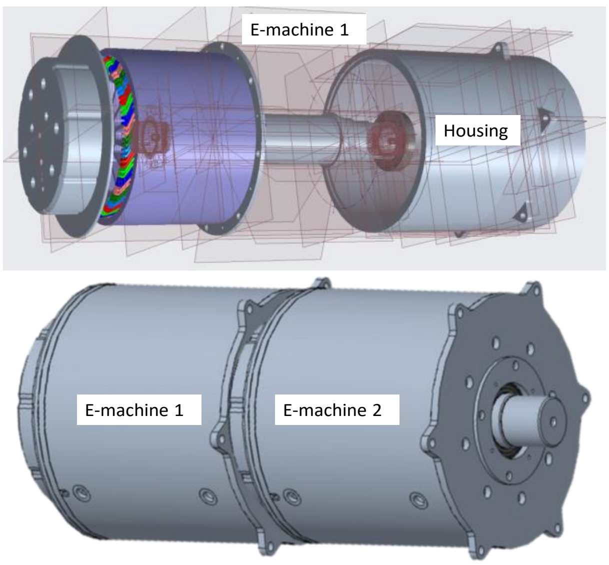

Fig. 8. Assembly of the individual components of E-machine 1 and mechanical design as stacked version for primary electric machine.

IV. Optimization possibilities

As an optimization option for this electric machine, there is, on the one hand, the introduction of new materials (sheet metal package with Cobalt and Halbach array). On the other hand, it is also possible to carry out the electromagnetic design with a genetic algorithm. In this section, the Halbach array and directly cooled stator windings are briefly explained in more detail. The Halbach arrangement of permanent magnets (PMs) is the combination of the radial and azimuthal PM arrangements. This combination results in a stronger magnetic field on one side of the arrangement, while the field on the other side cancels out to almost zero. That is why there is a big difference in the magnetic field around each magnet. Similarly, the thickness of the rotor laminations can be effectively reduced due to the concentration of the magnetic field without magnetically saturating the laminations, which in turn reduces the weight of the machine. Typically, the magnetic field is equally strong with a single magnet on both sides. For the Halbach arrangement, the magnets are arranged with all north poles facing upwards. From a magnetic point of view, this results in a single long magnet. The advantage of the Halbach arrangement is shown in Fig. 9. The arrangement of the magnets creates a powerful field on the upper side. On the lower side, the field strength lines almost cancel each other out or generate no field [18, 19]. Halbach arrays can be mainly divided into the straight type and circular type based on their geometry. Circular type can be further classified into outer diameter (O.D.) iteration and inner diameter (I.D.) iteration based on the arrangement of the permanent magnets. Numerous directions and strengths will be yielded by different magnet configurations. By deliberately changing the direction of the magnetization of the PM, further adjustments can be made to the magnetic flux distribution.

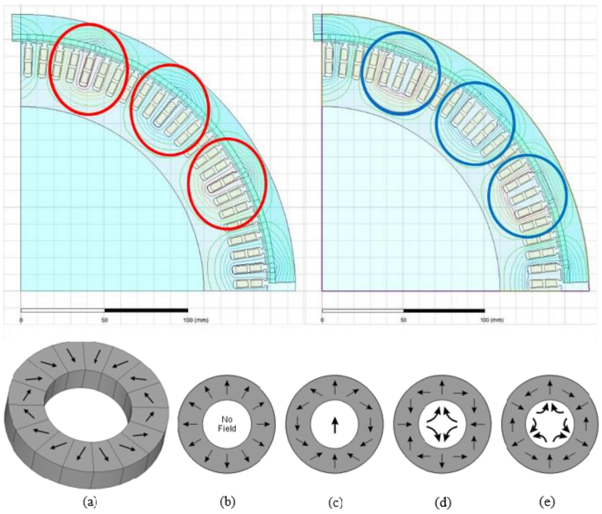

Fig. 9. Conventional magnet arrangement flux lines (left-red) and Halbach array arrangement flux lines (right-blue) – ANSYS simulation - (a) Trapezoid magnets arrangement. (b) No magnet field in the center. (c) Focus magnetization at the center. (d) Less magnetization at center. (e) Magnetization focused on the edges of circle [20]

Fig. 9 illustrates the different arrangements of Halbach arrays. In Fig. 9 (a), all magnetization directions are outwards. No magnetic field is visible inside the magnetic ring. In contrast, a magnetic field is present inside the magnetic ring in Fig. 9 (b), (c) and (d) and has a different number of pole pairs, namely 1, 2 and 3, respectively [20]. According to numerical calculations, and harmonic analysis, the PMSM with Halbach magnet array provides higher torque and better performance than the classical radial PMSM [18, 20]. In addition, Halbach arrays offer other advantages like: (i) they have excellent magnetic field performance when certain gaps exist, (ii) their magnetic field exhibits sinusoidal distribution and drastically reduces harmonic waves, (iii) they provide an effective increase in power and (iv) they provide an excellent magnetic shielding effect.

Due to the increasing demands on electrical machines, new cooling concepts have to be designed, so for some time now the focus has been on direct cooling concepts. These concepts aim to shorten the existing heat path through the machine by cooling as directly as possible at the heat sources in the machine, usually the copper or aluminum windings and the stator laminations, thus improving the overall machine efficiency. For directly cooled stator windings, two methods should be widely used so far: (i) winding head and stator cooling by cooling medium flowing around the winding, concept aiming at a total cooling of the large loss sources, since the entire stator, including the winding, "floats" in the dielectric; (ii) winding cooling by hollow wires or other conductor geometries.

By using hollow copper wires for the stator winding, which carry the cooling medium, this concept can also be used to cool the winding directly. Other geometries are possible from the hollow wire, like the ones in Fig. 10. [21–23]. First, a type-8 stranded coil with a rectangular shape is presented. The windings are filled with a highly heat-conductive potting material. The same applies to the stator slots. However, heat dissipation is limited by the thermal conductivity of the potting material and the surrounding slot insulation. This concept can be modified by inserting cooling channels into the potting material, as shown on the left in Fig. 10 (1). In the same figure (2) the stranded winding can also be cooled directly by wrapping the winding around the outside of a rectangular metallic cooling channel. This approach brings the strands in close thermal proximity to the coolant while maintaining the AC losses of the stranded construction. This type of stranded coil configuration is manufacturable with some trade-offs. The cooling channel has two important tasks in this configuration: it transfers heat from the stranded coils to the coolant and provides structural support for the strand winding and coolant flow. The metallic cooling channel is also exposed to, among other things, fluctuating alternating fields from the magnetic field within the stator slots. This can cause considerable eddy currents and Joule losses. In addition, the cooling channel takes up valuable space in the coil area, reducing the copper fill factor and increasing the DC electrical resistance and copper losses. Therefore, the duct must be thoughtfully designed to minimize the cross-sectional area required for its walls while balancing structural strength, thermal conductivity, and electrical resistance. Stainless steel, for example, is a good material for this. The total losses of the winding are usually estimated to be twice higher than those for the type 8 stranded coil. However, this approach with the core channel achieves a much lower thermal resistance, which reduces the winding temperature despite the higher losses. The third cooling option is shown in Fig. 10 (3). This solution uses a solid rectangular copper channel as a conductor with internal coolant flow. This allows an impressively low thermal resistance to be achieved, as the coolant is in direct contact with the walls of the conductor over the entire length of the channel. The copper fill factor is also higher than with the combination of stranded wire and core cooling channels (1) and (2), which reduces the DC resistance. As a disadvantage, it should be mentioned that the AC losses associated with the solid-wall channel are significantly higher due to the high operating frequency and the spatial harmonic content of the concentrated winding distribution. According to FEA estimates, the total losses of the solid copper concept are approximately five times higher than the losses of the stranded coil type 8 [22, 23].

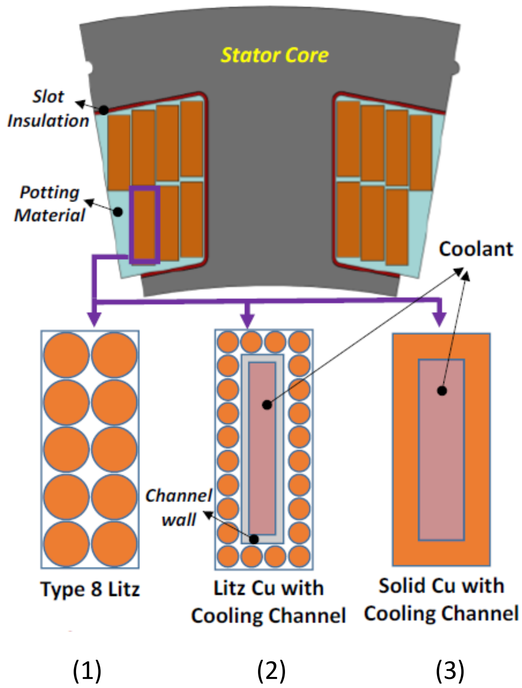

Fig. 10. Cross section of electric machines stator slot [22, 23]

V. Conclusions

This paper has presented an electric machine for a 50 PAX hybrid-electric aircraft. The engine concept presented can realistically achieve market entry in 2025 with the time required to qualify and set up series production. The results shown included the arrangement of the engine on the aircraft, a brief explanation of the powertrain and a detailed description of the design process of this electric machine. The power density of this motor meets the requirements for integration in a regional aircraft. Furthermore, the paper has discussed various optimization possibilities for the presented machine design. A Halbach magnet arrangement can achieve a more sinusoidal magnetic field in the air gap compared to a conventional PMSM. The magnetic field density in the air gap is increased, and iron losses are reduced. With directly cooled copper windings, the current density and, thus, the power density can be increased. The higher current density can lead to higher ohmic losses and, thus, lower motor efficiency. Therefore, a differentiated investigation of these two optimization options is necessary. Further optimization of the primary electric machine can also be achieved by designing a new motor housing enclosing two secondary machines' active parts.

VI. REFERENCES

[1] O. Zaporozhets, V. Isaienko, and K. Synylo, "PARE preliminary analysis of ACARE FlightPath 2050 environmental impact goals," *CEAS Aeronaut J*, vol. 12, no. 3, pp. 653–667, 2021, doi: 10.1007/s13272-021-00525-7.

[2] Bruno Lemoine Thomas Wannemacher NilsBaumann Alexe Guiguemde Zhangqi Wang, Mario Distasio Manuela Ruocco, Christian Bentheimer, "Short-term technology analysis covering all main," https://www.genesis-cleansky.eu/deliverables.

[3] A. Laurent, *GENESIS-The Project.* Accessed: 02 08 2022. [Online]. Available: https://www.genesis-cleansky.eu/the-project/

[4] magniX-The Electric Solution. Accessed: Feb. 13 2023. [Online]. Available: https://www.magnix.aero/services

[5] EMRAX d.o.o., "STACKED MOTOR – EMRAX TWIN," Accessed: Feb. 13 2023. [Online]. Available: https://emrax.com/e-motors/stacked-motor/

[6] Markus Meindl (FAU-LEE), Bruno Lemoine (BFH), Dr. Priscilla Caliandro (BFH), Dr. Erdem Akay (TUD), Sergio Turteltaub (TUD), Thomas Wannemacher (PMFC), Dr. Nils Baumann (PMFC), Alexe Guiguemdé (MHT), Mario Di Stasio (UNINA), Manuela Ruocco (SMARTUP), Fabrizio Nicolosi (UNINA), Agostino De Marco (UNINA), Pierluigi Della Vecchia (UNINA), "Medium-term technology analysis covering all main technologies in T2.1 - T2.6," May. 2022. Accessed: Jan. 18 2023. [Online]. Available: https://www.genesis-cleansky.eu/deliverables/

[7] "Comparative Analysis and Optimization of Technical and Weight Parameters of Turbo-Electric Propulsion Systems," *Aerospace, vol. 7, no. 8*, p. 107, 2020.

[8] T. Jokinen, V. Hrabovcova, and J. Pyrhonen, *Design of rotating electrical machines*: John Wiley & Sons, 2013.

[9] Prof. Dr-Ing. Ingo Hahn, "Vorlesung Elektrische Maschinen I," Vorlesung an der Friedrich-Alexander Universität Erlangen-Nürnberg, Elektrische Antriebe und Maschinen, Friedrich-Alexander Universität Erlangen-Nürnberg, Erlangen. Accessed: 2020.

[10] W. Tong, *Mechanical design of electric motors*. Boca Raton, Florida: CRC Press, 2014.

[11] E. Bolte, "Auslegung von elektrischen Maschinen," in *Elektrische Maschinen*: Springer, 2018, pp. 601–667.

[12] Ansys, "Ansys Electronics Electromagnetic, Signal Integrity, Thermal and Electro-Mechanical Simulation Solutions," Accessed: Feb. 13 2023. [Online]. Available: https://www.ansys.com/de-de/products/electronics

[13] PTC Inc., "Creo: Empower Your Design Team Today," Accessed: Feb. 13 2023. [Online]. Available: https://www.ptc.com/en/products/creo

[14] V. Marciello *et al.,* "Design Exploration for Sustainable Regional Hybrid-Electric Aircraft: A Study Based on Technology Forecasts," *Aerospace*, vol. 10, no. 2, p. 165, 2023, doi: 10.3390/aerospace10020165.

[15] Bruno Lemonie (BFH), Thomas Wannemacher (PMFC) Nils Baumann (PMFC), Alexe Guiguemde (MHT), Zhangqi Wang(ACC), Mario Distasio (UNINA), Manuela Ruocco(SMARTUP), Christian Bentheimer (FAU-LEE), "Short-term technology analysis covering all main technologies in T2.1 - T2.6: GAUGING THE ENVIRONMENTAL SUSTAINABILITY OF ELECTRIC AIRCRAFT SYSTEMS," 31.11.2021. [Online]. Available: https://www.genesis-cleansky.eu/deliverables/

[16] Andreas Binder, *Elektrische Maschinen und Antriebe: Grundlagen, Betriebsverhalten*. 9.4.2 Drehmomentwelligkeit von PM-Synchronantrieben, 2nd ed.: Springer Berlin Heidelberg, 2017.

[17] X. Liu, C. Bentheimer, F. Hilpert, M. Hofmann, B. Eckardt, and M. Maerz, "Digital Twin for a 10 MW Electrical Drive System for Future Electric Aircraft Applications," in *2021 11th International Electric Drives Production Conference (EDPC)*, 2021, pp. 1–9.

[18] Andy Yoon, Xuan Yi, Jon Martin, Yuanshan Chen, Kiruba Haran, "A High-Speed, High-Frequency, Air-Core PM Machine for Aircraft Application," in 2016.

[19] B. Ibtissam, "Magnetic Field Analysis of Halbach Permanent Magnetic Synchronous Machine," in *Proceedings of Engineering & Technology (PET)*, 2014, pp. 12–16.

[20] M. Meribout and S. Sonowan, "Optimal halbach magnet array design for portable NMR targeting multiphase flow metering applications," *IEEE Transactions on Magnetics*, vol. 55, no. 1, pp. 1–7, 2018.

[21] G.H.Byun, J.A.Kim, N.Y.Kim, Y.S.Cho, C.R.Park, "Molecular engineering of hydrocarbon membrane to substitute perfluorinated sulfonic acid membrane for proton exchange membrane fuel cell operation," Science Direct, https://www.sciencedirect.com/science/article/abs/pii/S2468606920301027?via%3Dihub.

[22] Dheeraj Bobba, Zhaoxi Yao, James Swanke, Raphael Mandel, Patrick McCluskey, Thomas Jahns, Bulent Sarlioglu, "Multi-Physics Based Analysis and Design of Stator Coil in High Power Density PMSM for Aircraft Propulsion Applications," in *AIAA Propulsion and Energy Forum*, 2021.

[23] Dr. Ing. Pouriya Ojahghlu, B. Eng. Björn Scheiffele, M. Sc Matthäus Brunner, Dr. Ing. Raad Al-Kinani, *Kühltechnologie für E-Maschinen neu gedacht So lassen sich E-Motoren über hohle Leitungen kühlen.* [Online]. Available: https://www.all-electronics.de/e-mobility/so-lassen-sich-e-maschinen-ueber-hohle-leiterbahnen-kuehlen-912.html (accessed: Dec. 7 2022).